The Iraqi Journal For Mechanical And Material Engineering, Vol.8, No.3, 2008

HEAT TRANSFER BY FREE CONVECTION BETWEEN HORIZONTAL CONCENTRIC PIPES

Dr. Tahseen A. Al-Hattab*, Dr. Majid H. Majeed **, and Mushtaq F. Abd-Saada*,
*Babylon University / Eng. College
**Al-Najaf Technical College

ABSTRACT

This research deals with the theoretical and experimental study of free convection heat transfer between horizontal concentric pipes of constant inner and outer cylinders temperature, respectively and (Ti>To). The finite elements method was used to solve the numerical relations of momentum and energy equations. The numerical solution has been included the calculation of the temperature and velocity values between the cylinders by using ANSYS program (finite element analysis structural system). Different models of concentric double pipes were created and tested with different diametral ratios. Nusselt number was obtained for a range of temperature difference (ΔT=Ti-To) of (6.01-120.42C0). The results also showed that the average heat transfer coefficient values at the inner and outer radii respectively increased with the increasing of Rayleigh number and the ratio of outer to inner radius. The theoretical and experimental results were compared with some of researches that presented in the literature to achieve the verification of the results obtained from the numerical analysis and experimental modeling for the heat transfer between concentric double pipes. The results are in good agreement.

الخلاصة:.

يتناول هذا البحث دراسة نظرية وعملية لانتقال الحرارة بالحمل الحر بين أنبوبين متحدي المركز بوضع أفقي بثبوت درجة الحرارة للأسطوانة الداخلية و الخارجية حيث تكون Ti>To. تم استخدام طريقة العناصر المحددة (Finite Elements) للحل العددي لمعادلات الزخم ومعادلة الطاقة الانتقالية. تضمنت الحلول العددية استخراج كل من توزيع درجات الحرارة، توزيع السرعة بين الأسطوانتين ومعادلات انتقال الحرارة باستخدام برنامج (Ansys) نفذ الحل العددي لنماذج متعددة وبنسب قطرية مختلفة.
بينت النتائج النظرية العملية بأن عملية انتقال الحرارة قد تمت بالتوصيل ($Ra<10^3$) حيث يكون رقم Nu اقل من (1). أما الانتقال بالحمل الحر يحدث عندما يصل رقم Ra لقيمة أعلى من 10^3 حيث يكون رقم Nu اكبر من (1). تم حساب رقم Nu لمدى معين لفرق درجات الحرارة ($\Delta T=T_i-T_o$) تبدأ من 6.01-120.42 (C^o) كذلك بينت النتائج أن قيم متوسط معامل انتقال الحرارة عند القطر الداخلي والخارجي على التوالي تزداد بزيادة رقم Ra ونسبة القطر الخارجي إلى الداخلي.

INTRODUCTION

Natural convection is observed as a result of motion of the fluid due to density changes arising from the heating process. A hot radiator used for heating room is one example of a practical device which transfers heat by free convection.[1].
In this study, the concentration will be on free convection "Free Convection Between horizontal concentric pipes". Flow in the annular region is characterized by two cells that are symmetric about the vertical mid plane. If the inner cylinder is heated and the outer cylinder is cooled (Ti >To), fluid ascends and descends along the inner and outer cylinder, respectively. If (Ti <To), the cellular flows are reversed.
The problem of the natural convection heat transfer in an annulus bounded by two horizontal cylinders has been a subject of intensive research years due to its wide technological applications, which ranges from nuclear reactors, thermal storage

systems, cooling of electronic components, aircraft fuselage insulation to underground electrical transmission lines, [2]. The problem is finding in insulating material that is transparent. An examination of the thermal conductivities of the insulating materials reveals that the air is a better insulator than most common insulating materials, besides it is transparent. Therefore, it makes sense to insulate the pipe with diameter greater than hot pipe (first pipe) to trap the air between two pipes. The results are an enclosure which is known as horizontal concentric double pipes in this case. Other example enclosure includes wall cavities, solar collector, cryogenic champers involving concentric cylinder or spheres, [3].]

Theoretical Analysis.

Finite Element Method (FEM) can also be useful in determining performance, especially conductivity gradients, temperature distribution, velocity profile. The heat transfer coefficient can be determined by using advance (ANSYS) (Analysis Structural Systems) codes which incorporate fluid mechanics.

Finite element Discritization.

The analysis guide manuals in the ANSYS documentation set describe specific procedure for performing analysis for different engineering disciplines.

A mesh is generated from the node of a "grid". The term grid is used in this work to define the set of nodal points, which puts up the respective mesh. Figure (1) shows proposed our finite element model (concentric double pipe), created by using two dimensional fluid elements (Fluid 141) of quadrilateral shape as shown in Fig (2)

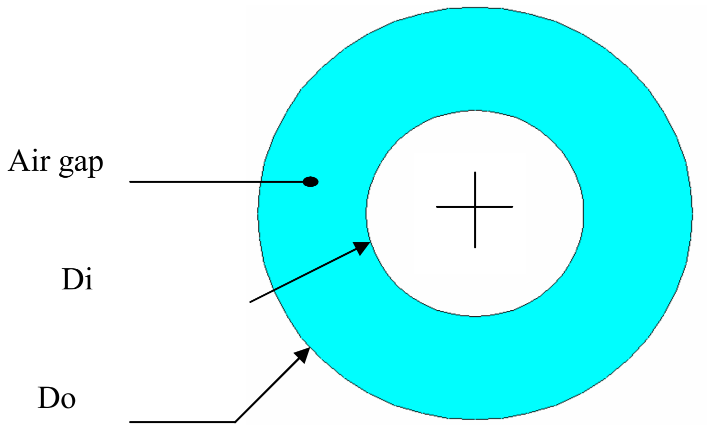

Fig.(1): Finite element modeling.

Mesh Generation.

Fluid 141 can be used to model a transient or steady state fluid/thermal systems that involve fluid and / or non-fluid regions. The conservation equations for viscous fluid flow and energy are solved in the fluid region, only the energy equation will be solved in the non-fluid region.

For the FLOTRN CFD element, the velocities are obtained from the conservation of momentum principle, and the pressure is obtained from the conservation of mass principle. (The temperature, if required, is obtained from the law of energy conservation.)

The specification of FLUD 141 according to ANSYS program can be shown as follow:

Element name	FLUID 141.
Nodes	I, J, K, L.
Degree of freedom	Vx, Vy, PRES, TEMP, ENKE, ENDS.
Surface load	HFLUX, CONV, RAD.
Body loads	HGFN, FORC.

.

And the shape function can defined as flow:

$\Phi = N_1\Phi_1 + N_2\Phi_2 + N_3\Phi_3 + N_4\Phi_4$

Where Φ : the degree of freedom.

$N_1 = (1-s)(1-t)/4$

$N_2 = (1+s)(1-t)/4$

$N_3 = (1+s)(1+t)/4$

$N_4 = (1-s)(1+t)/4$

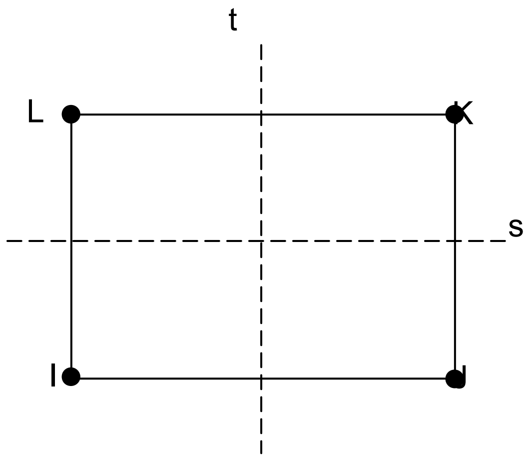

Fig.(2): Quadrature two-dimension element

ANSYS finite element program is used in the theoretical analysis of this model, according to the following steps: (1) the inner diameter cylinder is 23mm and the outer diameter cylinder is following values (46, 50.6, 55.2, 59.8, 64.4 and 69) mm. This made $\delta / D_i = (0.5,\ 0.6,\ 0.7,\ 0.8,\ 0.9,\ and 1)$ where δ presents annulus gap width, and Di is the outside diameter of the inner cylinder. The region between concentric double cylinder (inner and outer cylinders) is discredited into 384 fluid elements of quadrilateral shape. Eight elements in the radial direction, and forty eight in the angular direction as shown in Fig.(3).

Governing Equations

In general, the governing equations for laminar, incompressible fluid flow can be given as shown in r, θ, z coordinates:-

Continuity Equation:

$$\frac{\partial \rho}{\partial t} + \frac{1}{r}\frac{\partial (rV)}{\partial r} + \frac{1}{r}\frac{\partial U}{\partial \theta} + \frac{\partial W}{\partial z} = 0 \qquad \ldots (1)$$

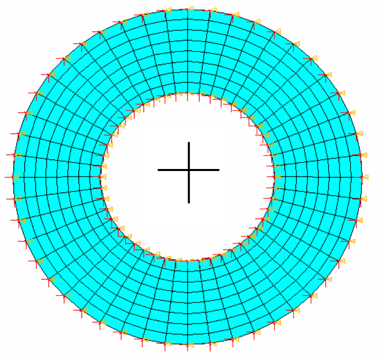

Fig.(3): Finite elements mesh generation and boundary condition.

2. Momentum Equation:

in r-direction

$$\rho\left(\frac{\partial V}{\partial t} + V\frac{\partial V}{\partial r} + \frac{U}{r}\frac{\partial V}{\partial \theta} - \frac{U^2}{r} + W\frac{\partial V}{\partial z}\right) = -\frac{\partial p}{\partial r} + \rho g_r$$
$$+\mu\left(\frac{1}{r}\frac{\partial}{\partial r}\left(r\frac{\partial V}{\partial r}\right) - \frac{V}{r^2} + \frac{1}{r^2}\frac{\partial^2 V}{\partial \theta^2} - \frac{2}{r^2}\frac{\partial U}{\partial \theta} + \frac{\partial^2 V}{\partial z^2}\right) \qquad \ldots (2)$$

in θ-direction

$$\rho\left(\frac{\partial U}{\partial t}+V\frac{\partial U}{\partial r}+\frac{U}{r}\frac{\partial U}{\partial \theta}+\frac{VU}{r}+W\frac{\partial U}{\partial z}\right)=-\frac{1}{r}\frac{\partial p}{\partial \theta}+\rho g_{\theta}$$
$$+\mu\left(\frac{1}{r}\frac{\partial}{\partial r}\left(r\frac{\partial U}{\partial r}\right)-\frac{U}{r^{2}}+\frac{1}{r^{2}}\frac{\partial^{2}U}{\partial \theta^{2}}+\frac{2}{r^{2}}\frac{\partial V}{\partial \theta}+\frac{\partial^{2}U}{\partial z^{2}}\right) \quad \ldots (3)$$

in z-direction

$$\rho\left(\frac{\partial W}{\partial t}+V\frac{\partial W}{\partial r}+\frac{U}{r}\frac{\partial W}{\partial \theta}+W\frac{\partial W}{\partial z}\right)=-\frac{\partial p}{\partial z}+\rho g_{z}$$
$$+\mu\left(\frac{1}{r}\frac{\partial}{\partial r}\left(r\frac{\partial W}{\partial r}\right)+\frac{1}{r^{2}}\frac{\partial^{2}W}{\partial \theta^{2}}+\frac{\partial^{2}W}{\partial z^{2}}\right) \quad \ldots (4)$$

3. Energy equation:-

$$\rho\,(V\frac{\partial T}{\partial r}+\frac{U}{r}\frac{\partial T}{\partial \theta}+W\frac{\partial T}{\partial z})=\frac{\mu}{p_{r}}(\frac{1}{r}\frac{\partial}{\partial r}(\frac{\partial T}{\partial r})+\frac{1}{r^{2}}\frac{\partial^{2}T}{\partial \theta^{2}}+\frac{\partial^{2}T}{\partial z^{2}}) \quad ...(5)$$

Assumptions and Boundary Conditions

The following assumptions which assumed for the system that consists of air bounded by two concentric annular spaces are: two dimensions (2-D) steady state system newtonian Fluid (air), the fluid is viscous and incompressible, frictional heating is negligible, the difference in temperature between the isothermal boundaries is small compared with the 1/β. The governing equations after simplification of continuity, momentum, and energy equations in two dimensions are shown as following (in r and θ coordinates):

1. Continuity Equation:

$$\frac{\partial V}{\partial r}+\frac{V}{r}+\frac{1}{r}\frac{\partial U}{\partial \theta}=0 \quad \ldots (6)$$

2. Momentum Equation:- (in r-direction)

$$\rho\left[V\frac{\partial V}{\partial r}+\frac{U}{r}\frac{\partial V}{\partial \theta}-\frac{U^{2}}{r}\right]=-\frac{\partial P}{\partial r}+\mu\left[\frac{\partial^{2}V}{\partial^{2}r}+\frac{1}{r}\frac{\partial V}{r}+\frac{1}{r^{2}}\frac{\partial V}{\partial \theta^{2}}-\frac{V}{r}-\frac{2}{r^{2}}\frac{\partial U}{\partial \theta}\right]$$
$$+g\rho\beta\,\left(T-T_{O}\right)\cos\theta \quad \ldots (7)$$

in θ-direction

$$\rho\left[V\frac{\partial U}{\partial r}+\frac{U}{r}\frac{\partial U}{\partial \theta}+\frac{VU}{r}\right]=-\frac{1}{r}\frac{\partial P}{\partial \theta}+\mu\left[\frac{\partial^{2}U}{\partial r^{2}}+\frac{1}{r}\frac{\partial U}{\partial r}+\frac{1}{r^{2}}\frac{\partial^{2}U}{\partial \theta^{2}}-\frac{U}{r}+\frac{2}{r^{2}}\frac{\partial V}{\partial \theta}\right]$$
$$+g\rho\beta\,\left(T-T_{O}\right)\sin\theta \quad \ldots (8)$$

3. Energy equation:-

$$\rho\ c_p \left[V\frac{\partial T}{\partial r} + \frac{U}{r}\frac{\partial T}{\partial \theta} \right] = k \left[\frac{\partial^2 T}{\partial r} + \frac{1}{r}\frac{\partial T}{\partial r} + \frac{1}{r^2}\frac{\partial^2 T}{\partial \theta^2} \right] \quad \ldots(9)$$

Where,
V and U = components of the velocity vector in r and θ directions.
ρ = density
μ = dynamics viscosity
cp = specific heat
k= thermal conductivity.

$$g_r = g\beta(T_i - T_o)\cos\theta$$

$$g_\theta = g\beta(T_i - T_o)\sin\theta$$

The elliptic equations require that the boundary conditions be specified along the entire boundary conditions which enclose the flow field. The inner and outer cylinders are considered to be held at a uniform temperatures, Ti, and To, respectively such that Ti > To. The fluid velocity is zero on the wall of the pipes. It is assumed that at the lines of symmetry, the angular derivatives of the temperature are vanished.

Theoretical Calculation

The concentric double pipes are modeled by the tested dimensions that required in the Finite Element Method. Loads and boundary conditions are applied on the model. FLOTRN solver is used to exclude the results of temperature, velocity, and air properties in nodal coordinates system at each node. The results includes:

1-Calculation of mean temperature:

$$T_m = \frac{T_i + T_o}{2} \quad \ldots(10)$$

2- Calculation of local heat transfer coefficient:

The local heat transfer coefficient was calculated for the inner and outer cylinders at an orientation of (0, 45, 90, 135, and 180) by the following Equations:

$$-k\frac{\partial T}{\partial r}\bigg|_{r=r_i} = h_i(T_i - T_o) \quad \ldots(11)$$

$$-k\frac{\partial T}{\partial r}\bigg|_{r=ro} = h_o(T_i - T_o) \quad \ldots(12)$$

$$h_i = \frac{-k\frac{\partial T}{\partial r}\Big|_{r=r_i}}{(T_i - T_o)} \quad \ldots(13)$$

$$h_o = \frac{-k\frac{\partial T}{\partial r}\Big|_{r=ro}}{(T_i - T_o)} \quad \ldots(14)$$

3- Calculation of Nusselt number:

Nusselt number (Nu) presents the enhancement of heat transfer through a fluid layer as a result of convection relative to conduction a cross the same fluid layer. The larger Nu effective the convection. A Nusselt =1 for fluid layer represents heat transfer by pure conduction. Nusselt number at r_i becomes as:

$$Nu_{ri} = \frac{hi.(r_i \ln(r_o \ / r_i \ ))}{k}$$

$$Nu_{ro} = \frac{h_o.(r_o \ln(r_o \ / r_i))}{k} \qquad ...(16)$$

then, the mean Nusselt number is:

$$\overline{Nu} = \frac{\overline{h_o}.(r_o.\ln(r_o / r_i))}{k} = \frac{\overline{h_i}.(r_i.\ln(r_o / r_i))}{k} \qquad ...(17)$$

The heat transfer rate by convection becomes:

$$Q_{conv} = \overline{h_o} 2 * \pi * r_o (T_o - T_i) \qquad ...(18)$$

which is the mean of heat transfer coefficient at r2. Heat-transfer rate by pure conduction Qconv becomes:-

$$Q_{cond} = \frac{2 * \pi * k(T_i - T_o \ )}{\ln(r_0 / r_i)} \qquad ...(19)$$

4- Calculation of Rayleigh number:

$$Ra = \rho^2 g\beta\delta^3 (T_i - T_o) c_p /(\mu k)$$

where $\delta = (r_o - r_i)$

Experimental work

Experimental Model

The experimental models are mainly consisting of two cylinders, inner and outer. The inner is machined from solid stainless steel bar stocking into a tube 203mm long with an outside diameter of 23mm and a wall thickness of 3mm. This is heated by passing direct current through a 190 Ω tubular resistor approximately 180mm long held in the centre of the cylinder. 15 thermocouples distributed in the test section, 13 in the mid-plane spaced 45^{O} apart and one at each end of the test section (on the inner and outer cylinders surfers), were positioned within (3, 6 and 9) mm of the inner cylinder surface as shown in Fig.(4). Expanded solid cylinder of fire brick (17mm diameter and 11.5mm thickens) mounted on each end of the heater to reduce the conduction losses in the ends of inner cylinder. The inner cylinder is held concentrically within the outer cylinder by three wood disks with thickness 0.4cm and (23, 46) mm inner and outer diameter. The outer cylinder, also of stainless steel, is machined into a tube 20.35cm long with an inside diameter of 46mm and a wall thickness of 7.5mm. This made $\frac{\delta}{D_i}$ = 0.5, where δ is the annulus gap width and D_i is the outside diameter of the inner cylinder.

Cooling System

In order to attain constant temperature for the inner surface of outer cylinder (To=constant), the outer surface of this cylinder is cooled by circulated water of quasi-constant temperature. A simple cooling system is manufactured by using a third cylinder of radius of 75mm and 4mm in thickness, this cylinder is surrounded to the experimental model. This cylinder is provided with an input and output orifices to circulate the cooling fluid (water). Two orifices (upper and lower) are mounted at the third cylinder in order to ensure that the cooling system is good feature and efficiency. The constancy of outer cylinder temperature gives an approximation with the theoretical assumptions, thereby, an accordance to the experiments the results will be attained.

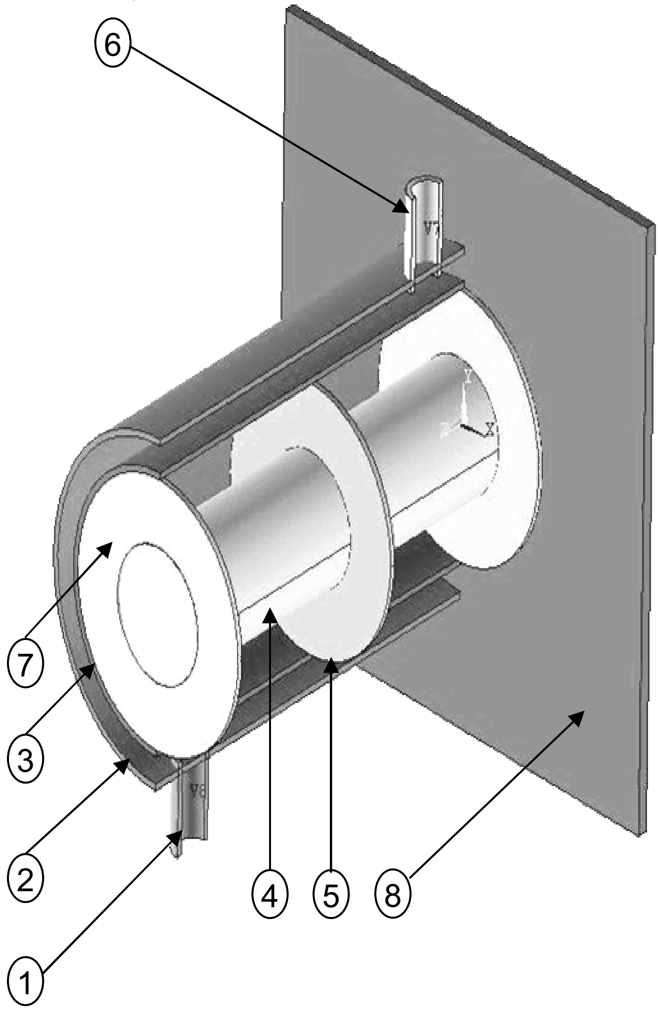

Fig.(4): Full geometrical consideration of the concentric pipes , 1- water inlet, 2- outer cooling cylinder, 3- outer pipe, 4- Inner pipe, 5- test section, 6- water outlet, 7-insulated discs, 8-handle

Thermocouple Sets

Thermocouple sets type K (0.27) mm Chromel-Alumel thermocouple wires are used. The thermocouple wire was cut into two pieces, each piece of the wire was skinned from both ends and one of the ends was spot-welded forming a spherical bead. In all experiments (15) thermocouples were distributed uniformly as shown in Fig. (5) in the air gap between the two cylinders and through their surfaces to determine the temperature distribution through these regions.

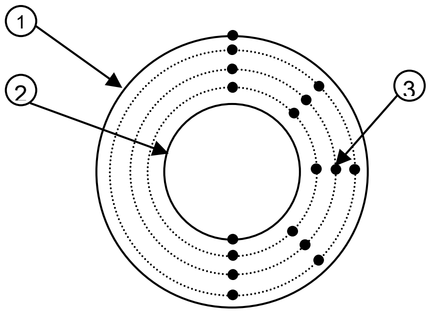

Fig.(5): Presents test section.1-outer cylinder, 2-inner cylinder, 3- thermocouples

Temperature Measurement

The temperatures are measured at the testing part that located in the middle section of the model as shown in the Fig.(5), so that the locations of the test are distributed in uniform manner to attain an wholly information about the temperature distribution through the section. Fig.(5) presents the distribution of thermocouples sets. There are 15 sets of these thermocouples, one insulated from the other through the experimental model. Two of them are located at the outer surface of the inner cylinder and the inner surface of the outer cylinder of the models and the other is distributed on a three circular paths around the inner cylinder of equally distance of 3mm from the inner cylinder of the model. At the first and the second circular paths, there are 5 sets of each set inclines from the other by 45°. But for the third path, there are 3 sets distributed in a 45°, 90°, and 180°.

RESULTS AND DISCUSSIONS

The experimental results represent the temperature distribution between concentric pipes for five levels and diameter ratio of (D=2). Because of the symmetry about Y-axis, the result would be appeared in a half model only. Where Fig. (6) shows the results on the rays angles with its levels. Ray (1), ray (2), ray (3), ray (4), and ray (5) are the location of the results presenting which are at angle (0°), (45°), (90°), (135°), and (180°), respectively.

Numerical Analysis

In this section, the numerical results of temperature distribution, Nusselt number, dimensionless radial temperature distribution, and velocity distribution are presented for a specific value of Rayleigh number and different boundary condition. Table (1) shows the result of calculation of mean temperature, Rayleigh number, inner and outer heat transfer coefficient and Nusselt number for different diameter ratios and boundary conditions.

Table (1a): Ra, $\bar{h}_i$, $\bar{h}_o$, and Nu at different theoretical Boundary Condition for(*D*=2).

ΔT(C°)	Tm(C°)	Ra	$\bar{h}_i$ (w/m^2.C°)	$\bar{h}_o$ (w/m^2.C°)	Nu
6.010	39.115	7.1E+02	3.1983	1.5991	0.96000
7.010	41.415	8.0E+02	3.4885	1.7442	1.01520
9.810	45.615	1.1E+03	3.6225	1.8113	1.04226
14.91	48.165	1.5E+03	3.7229	1.8615	1.06424
17.31	51.865	1.7E+03	3.8396	1.9198	1.08692
24.71	56.565	2.3E+03	3.8891	1.9445	1.08801
27.31	56.665	2.5E+03	4.1776	2.0888	1.16875
39.80	61.320	3.4E+03	4.3969	2.1985	1.21698
44.78	65.830	3.7E+03	4.4703	2.2352	1.22655
54.80	74.810	3.8E+03	4.6309	2.3155	1.23161
61.50	82.760	4.0E+03	4.7455	2.3727	1.24684
71.86	88.350	4.45E+03	4.7685	2.3843	1.25368
79.61	91.715	4.6E+03	4.9218	2.4609	1.26485

94.91	102.17	4.8E+03	5.1829	2.5915	1.30531
104.41	107.02	5.0E+03	5.3124	2.6562	1.32488
111.53	111.56	5.1E+03	5.4383	2.7192	1.34360
120.42	113.00	5.4E+03	5.5059	2.7529	1.35693

Table (1f): Ra, $\bar{h}_i$, $\bar{h}_o$, and Nu at different theoretical Boundary Condition for(D=3).

ΔT(C°)	Tm(C°)	Ra	$\bar{h}_i$ (w/m2.C°)	$\bar{h}_o$ (w/m2.C°)	Nu
6.010	39.115	5.7E+03	2.9291615	0.9764	1.36034
24.71	56.565	1.8E+04	4.31115	1.4371	1.91686
46.78	64.830	3.1E+04	4.4778428	1.4926	1.95855
61.50	82.760	3.2E+04	5.39276	1.7976	2.08190
77.61	92.715	3.6E+04	5.4365256	1.8122	2.23356
104.4	107.02	4.0E+04	5.752923	1.9176	2.29440
120.4	113.00	4.3E+04	5.8798293	1.9599	2.32120

Temperature Distribution

Fig.(7) shows the flow pattern at diameter ratio (D=2) for different values of Rayleigh number. The left half for all results represents the numerical results while the right half represents the experimental results for comparison purpose only.

The isotherms begin to resemble eccentric circles near Rayleigh number of 103 as can be seen from Fig. (7a, b, and c) and Fig.(8a), respectively. These regimes have been called (pseudo-conductive regimes) because the overall heat transfers coefficient has essentially for conduction state. Further increasing in Rayleigh number is showed in figures (c, d, e, and f) for figure(7) and Fig.(8), respectively, the temperature distribution becomes distorted which mean the overall heat transfer coefficient was increased. The boundary-layer thickness increases as the flow moves up around the cylinder. The largest thickness and smallest temperature gradient occur at the separation point on top. The buoyant plume above the inner cylinder impinges upon the outer cylinder at the top creating the thinnest boundary layer and highest heat flux for the system. This warm fluid then moves in a boundary layer adjacent to the outer cylinder towards the bottom. In part of the region between the two boundary layers a temperatures inversion exists, the fluid near the cool surface being warmer than that closer to the heated surface.

Dimensionless Radial Temperature Distribution

Fig.(9) presents the dimensionless temperature distribution for different Rayleigh number and diameter ratio. The trend of the distribution (temperature profile) at Rayleigh number near that 10^2 is quasi-linear the same behavior of thermal conductivity of an insulation between two walls (material insulation) which indicate that in this research the air between concentric double pipes behaves as a conductive insulation at small values of Rayleigh number as that verified previously,[4]. On the other hand, the global behavior for the curves is different with the variation in the position , i.e., the non-linearity of the these curves is increasing when the angular degree is different from 90° as shown above. In general, the divergence of the dimensionless radial temperature distribution increases with the increasing in the Rayleigh number that mentioned that an increasing in temperature gradient in the bottom and a decreasing in the top.

The effect of diameter ratio:- It is important to refer that for all figures {Figs. (9) and (10a)}, the increasing in the diameter ratio (D) from 2 to 3 will also increase the Rayleigh number which means that an increasing in the temperature values occurs. Taking fixed parameters Pr=0.7 and the same boundary condition (B.C), a variation in the diameter ratio (D) is made to examine its effect on the convection heat transfer for all figures above that represent temperature distribution along radial lines for diameter ratio (D)=2 and 3. The five different temperature curves and their slops have demonstrated that temperature curves and their slopes have increased angular dependence as the radius ratio is increased. The temperature inversion phenomena, that is the fluid layer near warmer surface becomes cooler than that near the colder surface for D=3

Velocity Distribution

Figures {Fig. (11) and Fig. (12)} show the variation of tangential velocity with dimensionless radius. One can see that, with assuming that the velocity has a positive value in the direction of the gravity acceleration (g) and negative in the opposite, the velocity closing to the inner cylinder (hot surface) are negative because the density of the hot air closing to hot surface is smaller than that corresponding to the cooling air. There are difference in the velocities values at different angular locations because these values are largely depends on the temperature gradient (temperature different) so that they maximum at 90° and minimum at 0° due the temperature differences. The inflection point of the curves from negative to positive values present a region of velocity values equal to zero (stagnation case).

The effect of diameter ratio on the velocity:- The increasing in the diametral values at the same Rayleigh number, will increase the temperature gradient for the same angular location, there by an increasing in the velocity value will increase also as shown in Fig. (13) at 90°. The effect of Rayleigh number on the velocity:- The increasing in the Rayleigh number leads to tangential velocity that resulted from increasing the temperature gradient as shown in Fig. (14) at 90°.

The effect of Rayleigh number and diametral ratio at same angular location (90°):- The tangential velocity has maximum and minimum values at the same radial location and zero at the middle point of the radial displacement (stagnation region), the value of each tangential velocity is different depending on the Rayleigh number and diametral ratio as shown in the Fig.(15)

Fig. (16) Presents the velocity distribution between concentric duple pipes at different Rayleigh number and diametral ratio. A better understanding for this distribution is arising from diametral and Rayleigh effects as shown in Fig.(16) (a, b, c, and d). Velocity values are increased with the increasing in Rayleigh number and diametral ratio. The maximum velocity occurs in region that follows the inner cylinder boundary layer and decreased to zero at the outer boundary layer attached to outer cylinder. A stagnation region is presented at the location of zero velocity at the top and bottom of each cylinder. The stagnation regions are largely depending on the Rayleigh number so that they increased with the increasing of Rayleigh number.

Nusselt Number in Concentric Double Pipes

Nusselt number represents an important coefficient of free convection heat transfer. Generally, Fig. (17) presents the relation between Nusselt and Rayleigh number. Nusselt number is shown to be increased in a quasi-linear form with the increasing of Rayleigh values because of the non directory dependence on the Rayleigh, so that Nusselt number is a function of heat transfer coefficient (h), and thermal conductivity (k), and diameter ratio (D) that represent an efficient parameter to evaluate Rayleigh number. The comparison between the theoretical results of the present work and {Yunus, K&G(Kuehn and Goldstein), B&C(Buchberg and Catton), and VDI}[5] shows a good agreement. The differences between the results are caused by the difference in getting of the average properties of working fluid.

Experimental Results

Temperature Distribution

The right halves of figures from {Fig.(7a) and (8a)} represent the experimental results from the comparison between the theoretical and experimental results shows a good agreements between them. The small differences between the results are caused by round off-error that resulted from all experimental auxiliary tools (interphase, power supply, thermocouple, etc…).

Dimensionless Radial Temperature Distribution

As a general view of the figures of experimental and theoretical results from {Fig. (9) and (10)}, where experimental results is presented the right halve side, for the same boundary condition they have a same behavior with small differences. The discrepancy in the numerical result arises from that the experimental results is taken as an average magnitude for the whole model which is different from the theoretical that the average magnitude is taken for each regions, the finite number of nodes, the convergence level of the solution and the necessity to cross plot the results.

Nusselt Number in Concentric Double Pipes

There is a good accordance between the experimental and theoretical results so that the results present the same behavior and the same of variation resulted from physical properties and condition of experimental test. Fig. (25) shows the comparition.

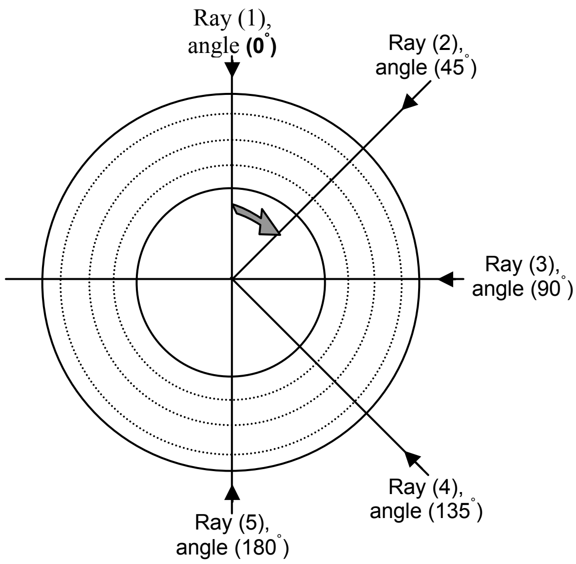

Fig.(6): Sections of the presented results.

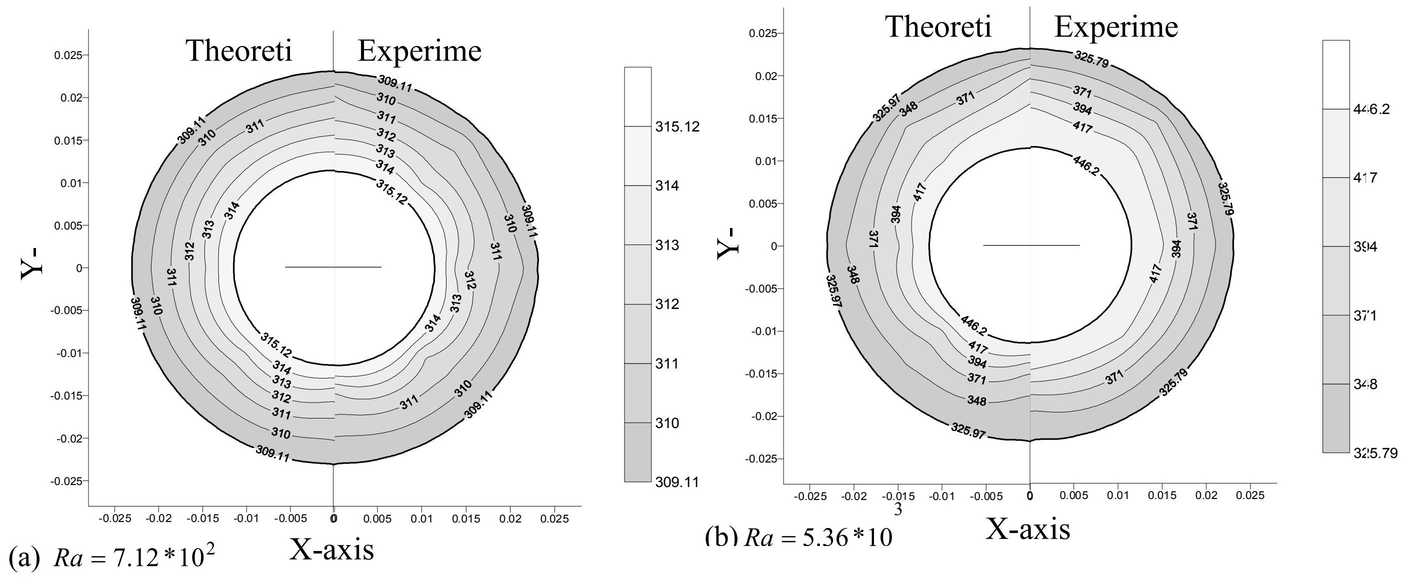

Fig. (7): Effect of Variation of Ra on (temperature) isotherm at *D*=2.

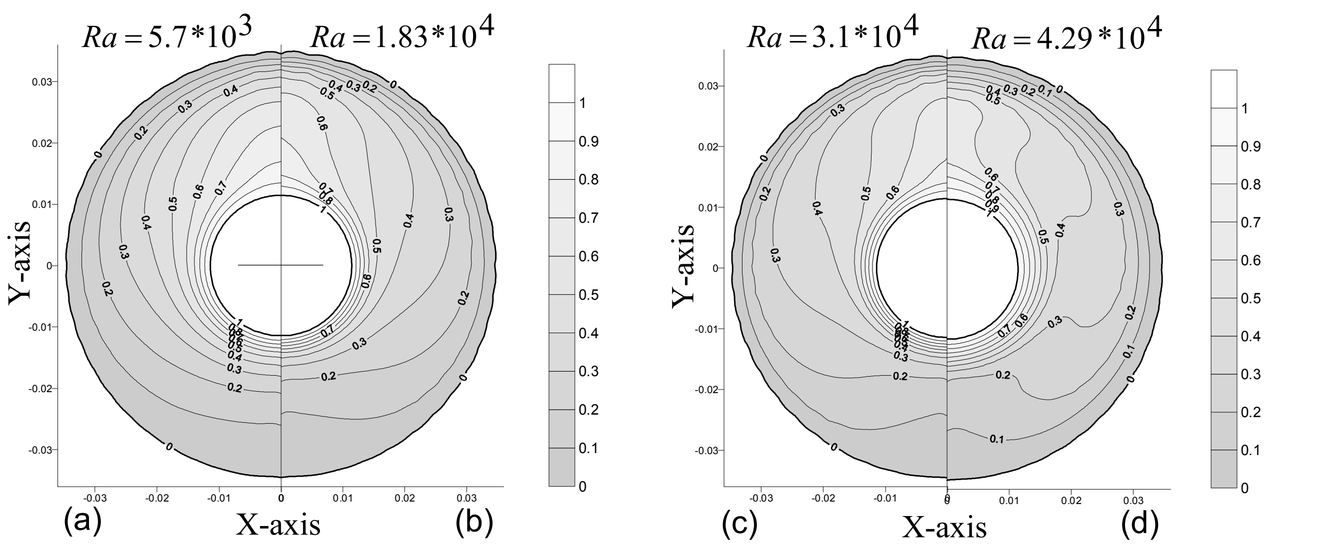

Fig. (8): Effect of Variation of Ra on (temperature) isotherm at *D*=3

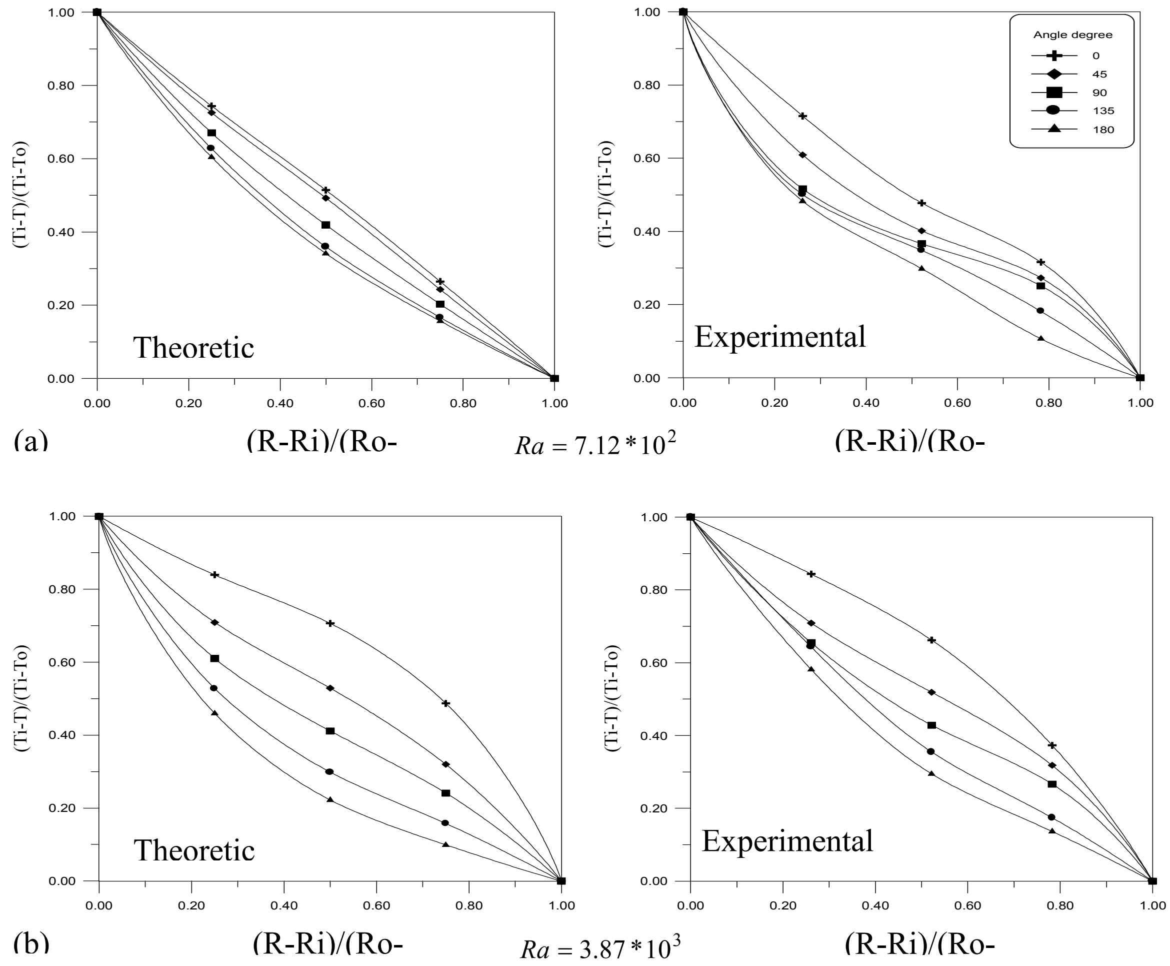

Fig. (9): Dimensionless radial temperature distribution at *D*=2

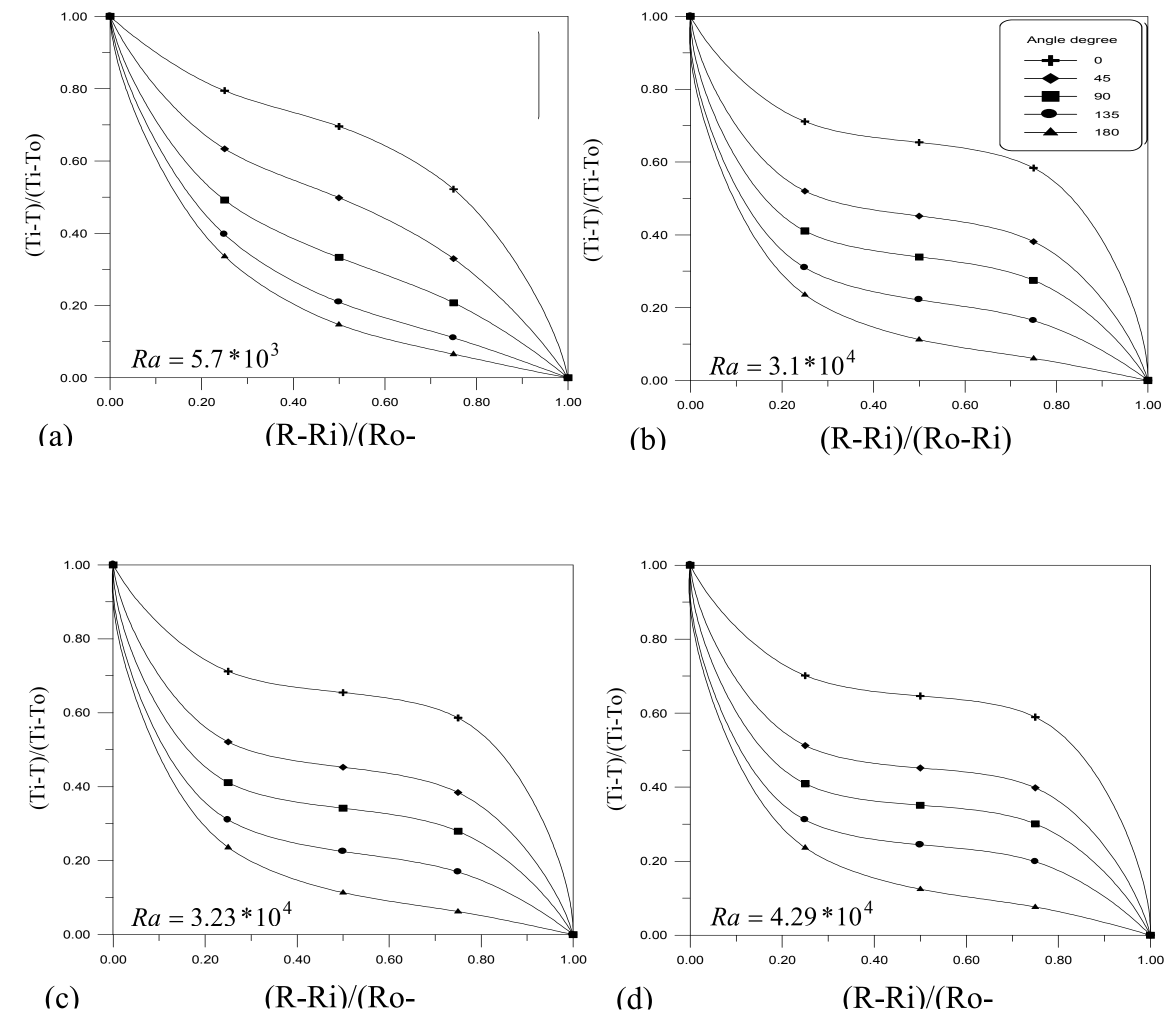

Fig. (10): Dimensionless radial temperature distribution at *D*=3

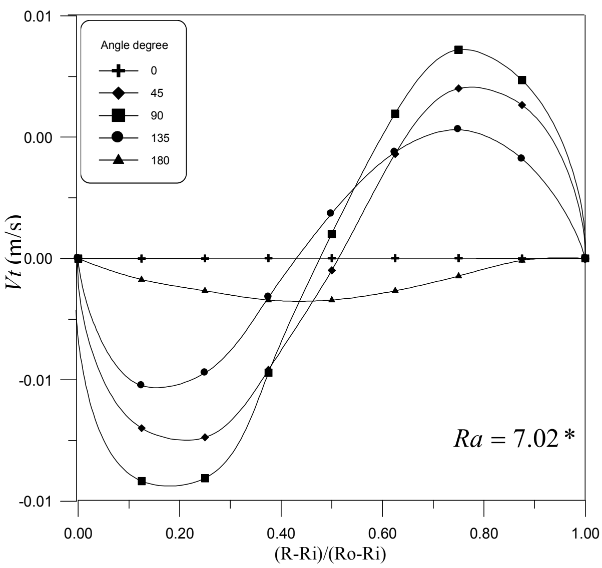

Fig. (11): Tangential velocity at *D*=2.

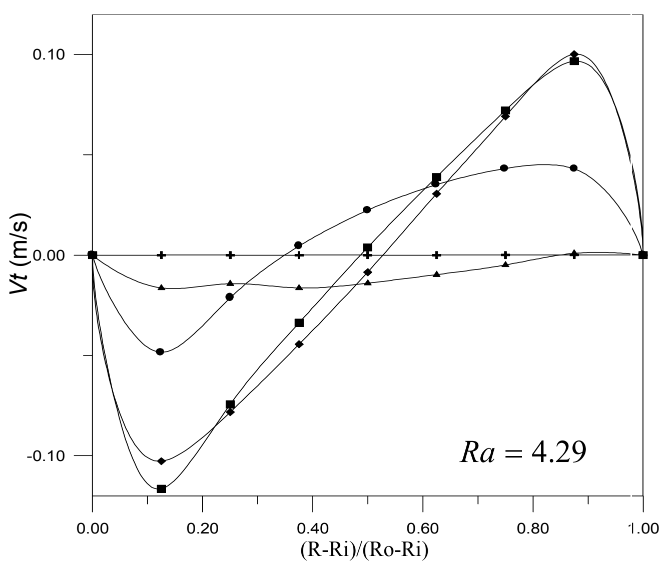

Fig. (12): Tangential velocity at *D*=3

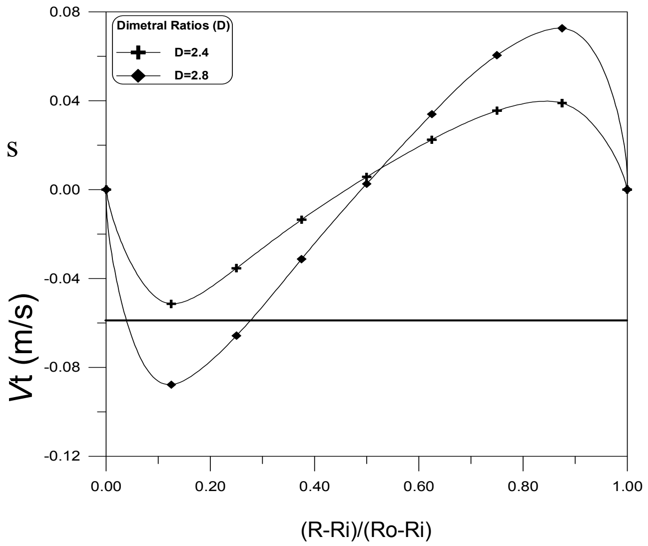

Fig.(13): Tangential velocity at different dimetral ratios and Ra=1.33*10^4 at θ=90^o.

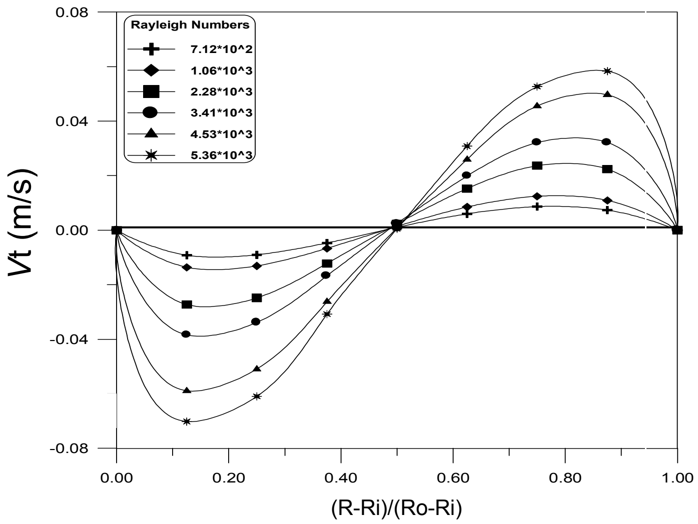

Fig.(14): Tangential velocity at different Rayleigh numbers for D=2 at θ=90^o.

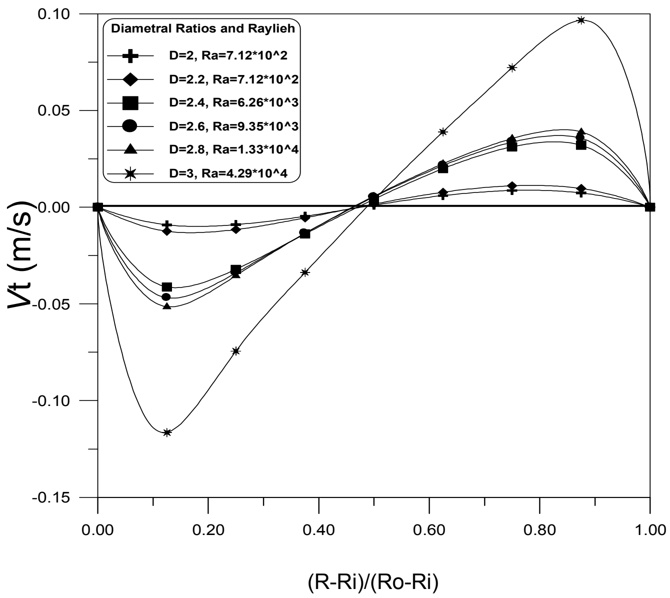

Fig.(15): Tangential velocity at different Rayleigh numbers and dimetral ratios at θ=90^o.

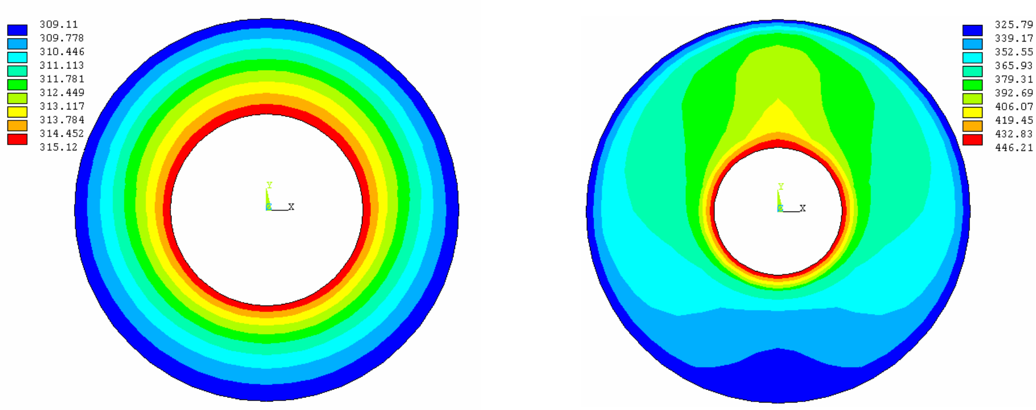

(a): Ra= $7.12*10^2$, D= 2 (b): Ra= $4.29*10^4$, D= 3

Fig. (16): Temperature distribution through air gap for different diametral ratios and Rayleigh numbers.

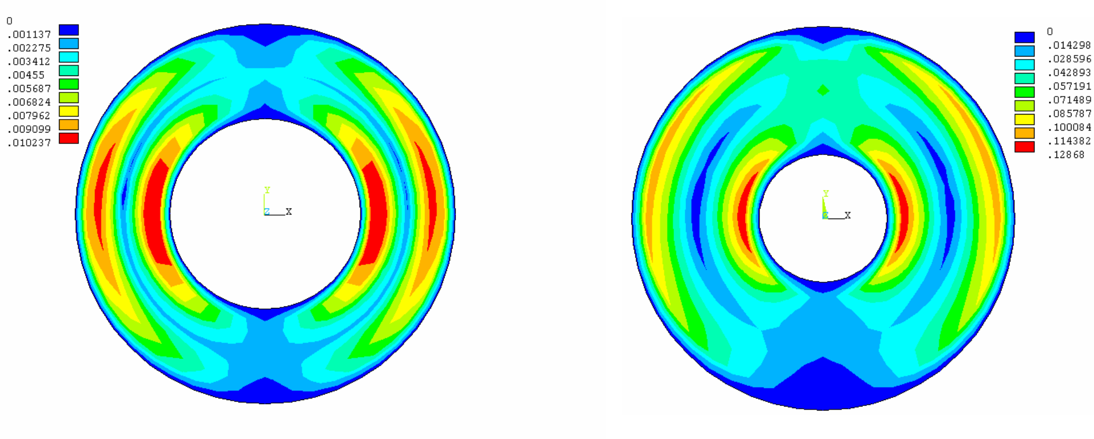

(a): Ra= $7.12*10^2$, D= 2 (d): Ra= $4.29*10^4$, D= 3

Fig. (17): Velocity distribution through air gap for different diametral ratios and Rayleigh numbers.

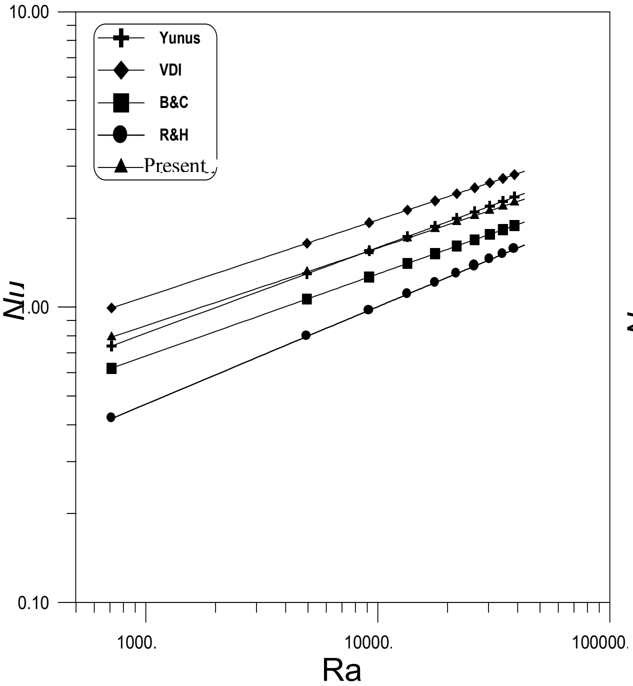

Fig. (18): Dimensional analysis of the field test and comparison with various correlations.

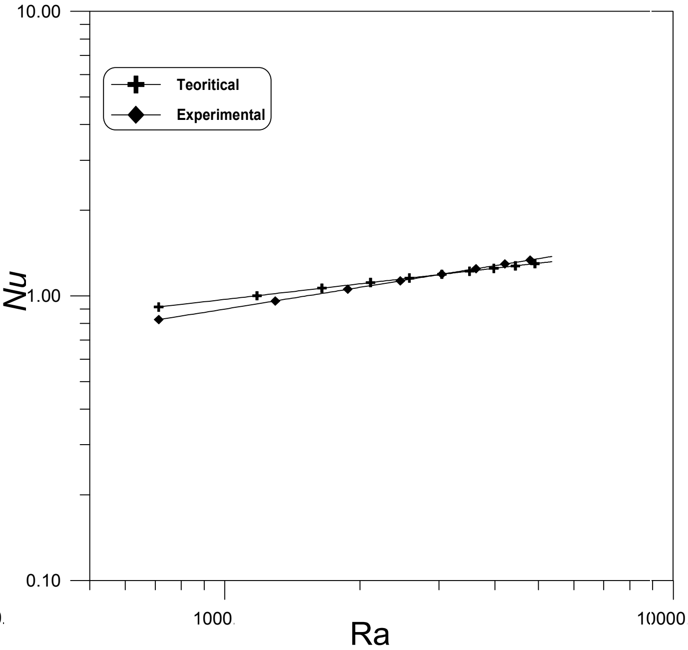

Fig. (5.25): Comparison of experimental and theoretical Nusselt number.

Conclusions.

It is concluded that, air can be used as an excellent insulator due to the smaller thermal conductivity than that corresponding of the other metals in addition to low unit cost. Conduction heat transfer through air gap occurs at a Nusselt number is less and equal than one and Rayleigh less than 10^3, while convection heat transfer (free convection) occurs at Nusselt number is greater than one and Rayleigh greater than 10^3. There are excellent agreements between the experimental and theoretical results. The insulation regions may be recognized with the stagnation, inner boundary layer, outer boundary layer, core region, and plume regions, respectively. The stagnation region became more pronounced with the increasing of Rayleigh number (Ra) in the top region between the inner and the outer boundary layers for the inner and outer pipes, respectively. The tangential velocity occurs at 90°, so that it increases from the zero and increases to the maximum value and then increases at zero again to reach a maximum beside the boundary layer of the inner cylinder and at last decreasing at the wall of the cylinder to the zero. The tangential velocity increases with the increasing in the Rayleigh number. Heat transfer coefficient increases of with the increasing of Ra and the air gap. Rayleigh number increases with the increasing of the diametral ratio for the same boundary conditions. The flow deformation became more pronounced with the increasing of Rayleigh number, thereby, closing to the turbulent manner with the increasing of Rayleigh number occurs.

References.

1. **Jischke, M. C. and Farshchi, M**. "Boundary Layer Regime for Laminar Free Convection between Horizontal Circular Cylinders". ASME Journal of Heat Transfer, Vol.102, pp.228-235, (1980).

2 Tsui, Y. T. and Tremblay, B. "On Transient Natural convection Heat Transfer in the Annulus Between Concentric Horizontal Cylinders with Isothermal Surfaces". Int. J. Heat Mass Transfer, Vol. 1. pp.103-111, (1983).

3. **Yunus, A. C.** " Heat Transfer: A practical Approach". McGraw-Hill, New York, (1997).

4. Kuehn, T. H. and Goldstein, R. J. " Correlating Equations For Natural convection Heat Transfer between Horizontal Circular Cylinders".

5. Clemes, S. B.; Hollands, K. G. T. and Brunger, A. P. " Natural convection Heat Transfer From Long